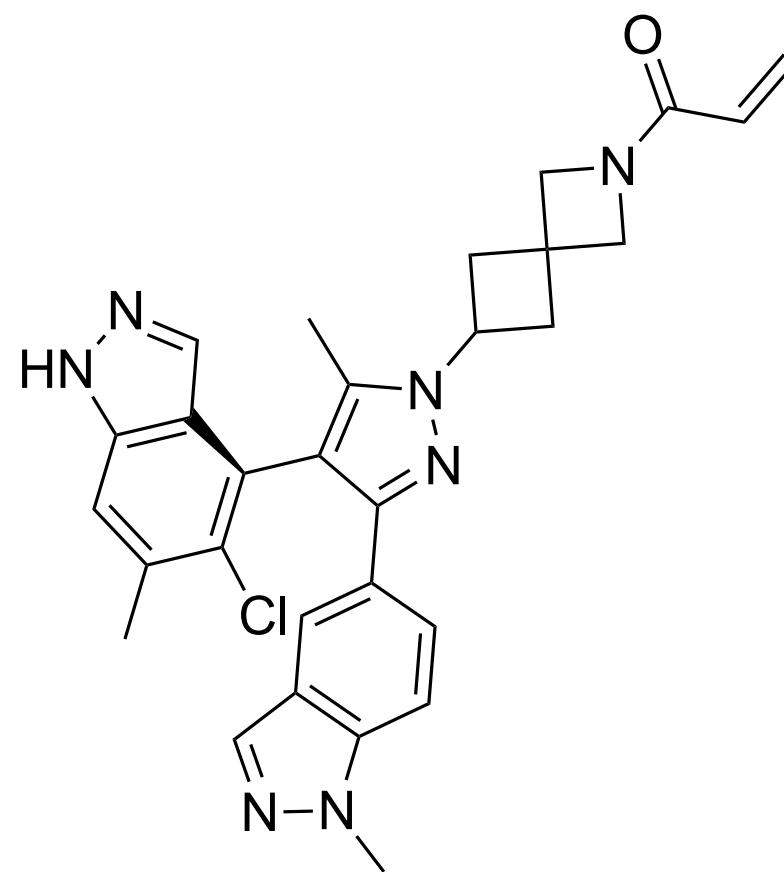


# Small Molecules of the Month

April 2022

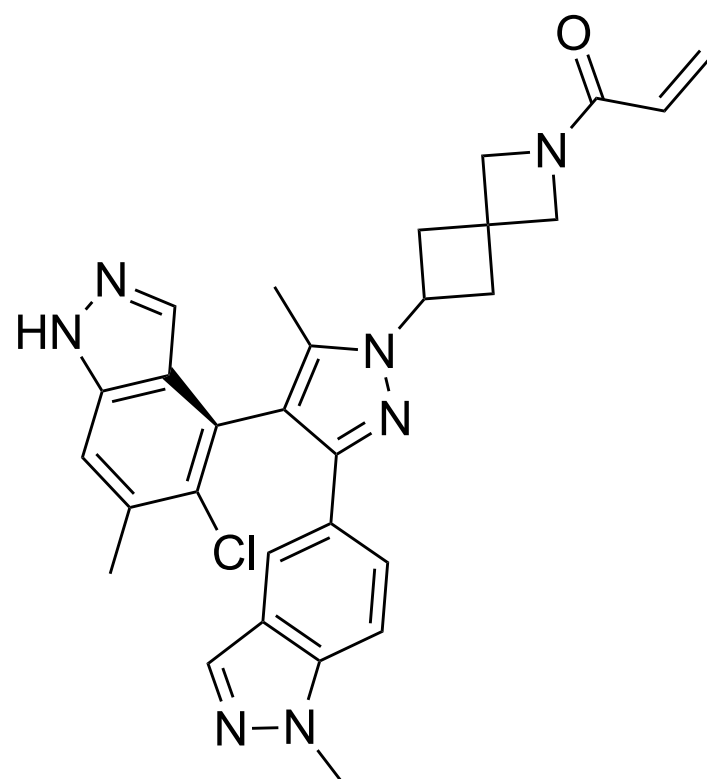
drug  
hunter



<b>01</b>	<b>JDQ443</b>	<b>Novartis</b>
<b>02</b>	<b>AZD4625</b>	<b>AstraZeneca</b>
<b>03</b>	<b>JBj-09-063</b>	<b>Dana-Farber Cancer Institute</b>
<b>04</b>	<b>ABBV-318</b>	<b>AbbVie</b>
<b>05</b>	<b>tenapanor</b>	<b>Ardelyx Inc.</b>
<b>06</b>	<b>lenrispodun</b>	<b>Intra-Cellular Therapies</b>
<b>07</b>	<b>compound 41</b>	<b>Vanderbilt University School of Medicine</b>
<b>08</b>	<b>DS69910557</b>	<b>Daiichi Sankyo</b>
<b>09</b>	<b>compound 14</b>	<b>Shionogi</b>
<b>10</b>	<b>compound 53</b>	<b>University of Texas Southwestern Medical Center</b>

# JDQ443

KRAS<sup>G12C</sup>



oral KRAS<sup>G12C</sup> inhibitor

Ph. III candidate for NSCLC

from de novo SBDD in SWII pocket

Cancer Discov.

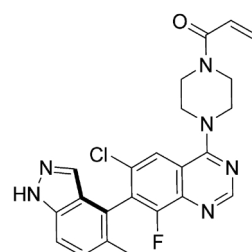
Novartis, Basel, CH

**Context.** [JDQ443 \(Novartis Institute for Biomedical Research\)](#) is an oral KRAS<sup>G12C</sup> inhibitor being developed for various advanced solid tumors. Despite accounting for [85% of RAS oncogenic mutations](#) in all cancers, KRAS was considered undruggable until 2013 when a [report](#) describing the targetability of the KRAS<sup>G12C</sup> mutant by small molecule inhibitors launched the oncogene back into the cancer research limelight. It is currently one of the [highly pursued cancer targets](#), with Amgen's KRAS<sup>G12C</sup> inhibitor, the first-in-class [sotorasib \(Lumakras\)](#), gaining [recent approval](#), and Mirati's NDA for adagrasib [recently accepted by the FDA](#) based on [promising clinical data](#). Despite these advancements, emerging [data on acquired resistance to adagrasib and sotorasib](#) present a challenge that Novartis scientists [believe may be overcome with JDQ443](#), given the structural uniqueness of the molecule and its novel binding mode. Notably, [early clinical data are promising](#), and the compound's amenability to combination with other agents as demonstrated in preclinical studies is [currently being evaluated in a Ph. I/II clinical trial](#).

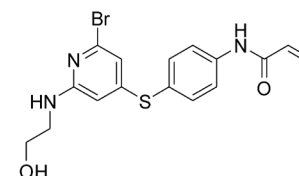
**Reviewer Comments.** Reviewer Callie Bryan says, "The Novartis JDQ443 compound uses the standard covalent paradigm with small molecules in clinical development but differs significantly in structure and binding. JDQ443 features two indazoles, one in the switch II pocket and the other is almost planar to the pyrazole core, occupying different regions of the pocket and exploiting new interactions. This leads to potent binding of the GDP-bound KRAS<sup>G12C</sup>."

**Mechanism of Action.** KRAS<sup>G12C</sup> inhibitors [typically](#) bind covalently to the mutated cysteine residue in a pocket that makes up the switch II region, locking the GDP-bound KRAS<sup>G12C</sup> in the inactive state and preventing reactivation by nucleotide exchange.

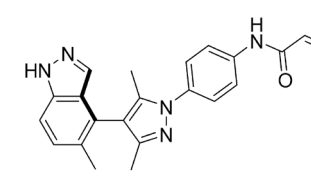
**Hit-Finding Strategy.** [The starting point for JDQ443 originated via de novo structure-based design inspired by the crystal structure of KRAS<sup>G12C</sup> bound to either a prior scaffold or a weak hit from an MS-based screen, in which the structural importance of the methyl indazole and the phenyl acrylamide groups were identified.](#) Subsequent *in silico* evaluation of novel scaffolds via covalent docking, including 5 or 6 membered aromatic as well as 5-6 fused aromatic moieties, to link the two groups led to the synthesis of starting point **compound 3**, which exists as a stable atropisomer.



known scaffold



weak MS hit

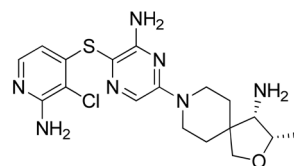


compound 3

**Lead Optimization.** Structure-activity relationship (SAR) analysis of compound 3 resulted in the replacement of the aniline linker with a spirocyclic azetidino moiety, decreasing promiscuous cysteine chemical reactivity and increasing specific KRAS<sup>G12C</sup> reactivity. Further optimization for specific reactivity for the target led to JDQ443.

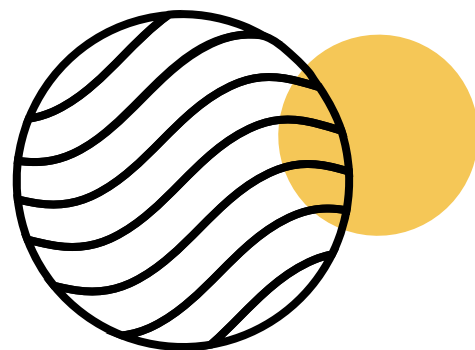
**Binding Mode.** The crystal structure of KRAS<sup>G12C</sup> in complex with JDQ443 (**PDB: 7RoM**) shows that the methyl-chlorine disubstituted indazole occupies a position between the switch II loop and the Gln-99 side chain, and forms a hydrogen bond with the backbone of the SWII loop, a water-mediated hydrogen bond with Ser-65, and a hydrogen bond with Asp-69. The methyl-substituted indazole does not appear to make H-bonding interactions, instead making stacking interactions with Gln-99 side chain and His-95. The rigid spirocyclic linker directs the acrylamide moiety to react with Cys-12. The oxygen atom from acrylamide forms a hydrogen bond with Lys-16 and a water-mediated interaction with a Mg<sup>2+</sup> ion bound to the GDP phosphates.

**Preclinical Pharmacology.** Biochemical and cellular assays demonstrated the potent inhibition of KRAS<sup>G12C</sup>-driven cellular signaling by JDQ443; the molecule also showed selective antiproliferative activity in KRAS<sup>G12C</sup>-mutated cell lines. *In vivo* studies were done in various KRAS<sup>G12C</sup>-mutated cell- and patient-derived xenograft mouse models. The molecule demonstrated dose-dependent inhibition at all tested doses across different indications and showed efficacy under both once- and twice-daily administration of the same dose. **Surprisingly** for a covalent inhibitor, the efficacy of JDQ443 was more driven by daily exposure, area under the curve (AUC) of JDQ443, and KRAS<sup>G12C</sup> target occupancy rather than the maximal concentration (C<sub>max</sub>) of JDQ443. The authors conducted a rigorous PK/PD assessment including measurement of target occupancy and KRAS<sup>G12C</sup> resynthesis rates in different cell lines to reach this conclusion, their description of which is worth a read. The activity of JDQ443 could theoretically be enhanced by co-administration with other agents that affect the RAS pathway. [Blockade of SHP2, an upstream oncogenic phosphatase, or MEK1/2 \(downstream\) may block RAS pathway reactivation resulting in prolonged KRAS<sup>G12C</sup> inhibition.](#) Indeed, when combined with SHP2, MEK, or CDK4/6 inhibitors, the activity of the JDQ443 was enhanced. Combination with the [SHP2 inhibitor TNO155 \(Novartis\)](#) increased *in vivo* target occupancy and delayed development of resistance, while the benefits of the combined regimen were consistent even at low doses of either agent.



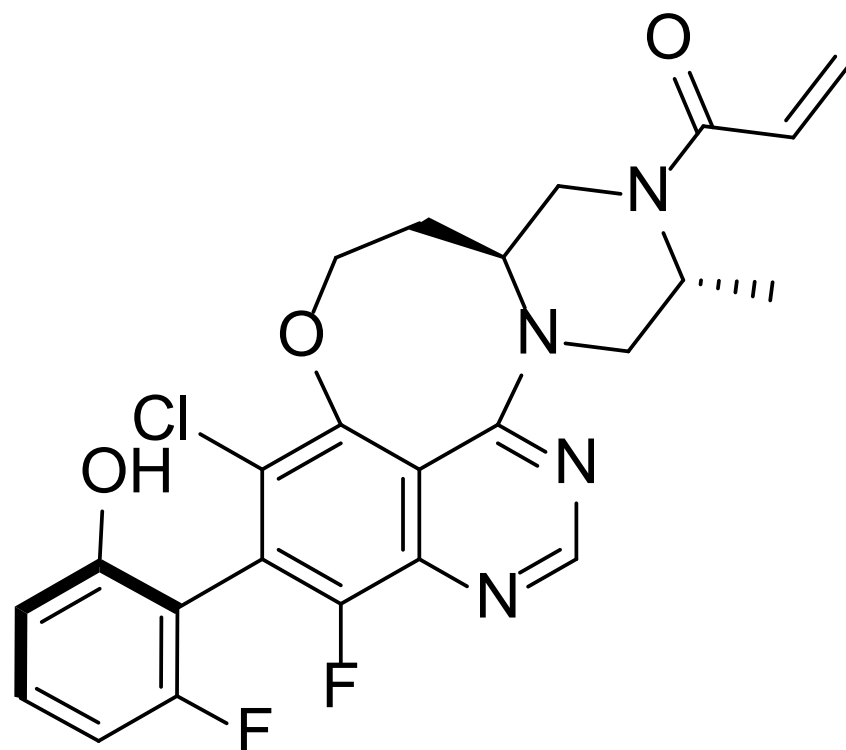
**TNO155**

**Clinical Development.** JDQ443 is currently being evaluated in the Ph. Ib/II KontraSt-01 trial ([NCT04699188](#)) for the treatment of advanced solid tumors harboring the KRAS<sup>G12C</sup> mutation. The safety and tolerability of JDQ443 as a single agent will be evaluated in a dose-escalation study in arm A of KontraSt-01. Arms B and C will evaluate JDQ443 in doublet combination with TNO155 (SHP2 inhibitor) and tislelizumab (a humanized IgG4 anti-PD-1 monoclonal antibody). Finally, arm D will evaluate the triplet combination of JDQ443, TNO155, and tislelizumab. Secondary outcome measures will include a dose-expansion study to assess the anti-tumor activity, the safety, tolerability, and PK/PD at the MTD and recommended dose. [Novartis recently disclosed promising early clinical data results from the KontraSt-01 trial.](#) JDQ443 demonstrated anti-tumor activity, favorable safety, and PK profiles with a T<sub>max</sub> of 3 to 4 hours following administration with food, and a half-life of 7 hours. In the subgroup of patients with non-small-cell lung carcinoma (NSCLC), who had received prior standard-of-care treatment or were ineligible for approved therapies, **an ORR of 57% was achieved with JDQ443 as a single agent at the RP2D of 200mg PO BID. No grade 4 or 5 TRAEs were reported** in these preliminary results. Another three clinical trials were launched by Novartis this year and are expected to start recruiting participants soon. A Ph. I ([NCT05329623](#)) study to evaluate the PK of a single dose of 200 mg JDQ443 in participants with hepatic impairment versus a healthy control group. A Ph. I/II ([NCT05358249](#) - KontraSt-03) study will evaluate the use of JDQ443 in doublet combination with trametinib (MEK inhibitor), ribociclib (CDK4/6 inhibitor), or cetuximab (EGFR targeted IgG1 monoclonal antibody). Lastly, a Ph. III study ([NCT05132075](#) - KontraSt-02) will compare JDQ443 as a monotherapy to docetaxel in participants with locally advanced or metastatic NSCLC harboring a KRAS<sup>G12C</sup> mutation who have been previously treated with platinum-based chemotherapy and an immune checkpoint inhibitor therapy, either in sequence or in combination.



# AZD4625

KRAS<sup>G12C</sup>



oral KRAS<sup>G12C</sup> inhibitor

oral efficacy in xenograft mice

from literature starting point and SBDD

*J. Med. Chem.*

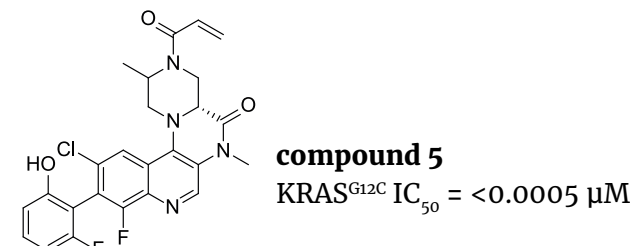
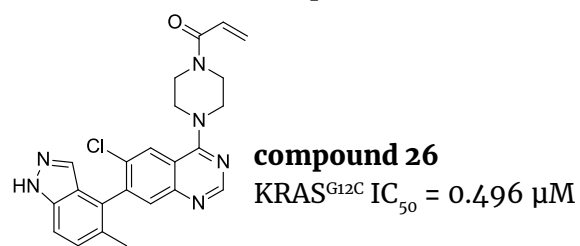
AstraZeneca, Cambridge, UK

**Context.** AZD4625 (AstraZeneca) is an oral inhibitor of KRAS<sup>G12C</sup> being developed for the treatment of advanced solid malignancies. As indicated for JDQ443, the KRAS<sup>G12C</sup> mutation presents the perfect “Achilles heel” for targeting a KRAS protein previously thought undruggable. The protein is a current hot topic in [precision oncology](#), with Amgen’s first-in-class [sotorasib \(Lumakras\)](#) having been approved, Mirati’s adagrasib [nearing approval](#), and other key agents such as [Genetech’s GDC-6036](#), [Eli Lilly’s LY3537982](#), [InvestisBio’s D-1553](#), and [Boehringer Ingelheim’s BI 1823911](#) all currently in early clinical development. AZD4625 is unique chemically, as it lacks a basic amine moiety that is typically carried by other KRAS<sup>G12C</sup> inhibitors, potentially exhibiting novel properties different from existing compounds. AZD4625 has not entered clinical evaluation yet (Ph. I study pending but not registered) and whether this new chemotype will clinically impact the highly competitive KRAS<sup>G12C</sup> space, where currently advanced molecules are dogged by acquired resistance, is unknown.

**Reviewer Comments.** Reviewer Callie Bryan says, “Similar to the Novartis JDQ443 compound, AstraZeneca’s AZD4625 also uses the standard covalent paradigm with small molecules in clinical development but differs significantly in structure and binding. AZD4625 potently inhibits KRAS<sup>G12C</sup> but through a quinazoline tethering strategy to lock out a bio-relevant binding conformation, and researchers addressed extrahepatic clearance. AZD4625 has an anticipated low clearance and high oral bioavailability profile in humans, and it will be interesting to see how these two strategies play out to benefit patients.”

**Mechanism of Action.** In typical KRAS<sup>G12C</sup> inhibition, binding of an inhibitor to the mutated cysteine in the allosteric switch II region locks the GDP-bound KRAS<sup>G12C</sup> in the inactive state which prevents reactivation of the protein. In AZD4625, a tether between the piperazine and quinoline groups improved the potency of the molecule by locking the active binding conformation of KRAS<sup>G12C</sup> which also reduced extrahepatic clearance mechanisms.

**Hit-Finding Strategy.** A selective covalent KRAS<sup>G12C</sup> potent inhibitor [was previously reported by AstraZeneca scientists](#). Starting from relatively weak inhibitor **compound 26**, described in a patent from Araxes Pharma ([WO2015054572](#)), a medicinal chemistry optimization campaign was conducted using experimental and computational techniques, leading to the discovery of potent and selective KRAS<sup>G12C</sup> inhibitor compound 5.



**Lead Optimization.** Applying a structure-based drug design approach combined with crystallographic analysis, resulted in AZD4625. The focus of the optimization was to reduce the extrahepatic clearance mechanisms observed in preclinical species. The addition of the methyl group on the tether piperazine ring reduced metabolism while maintaining potency. During the optimization process, computational solvent analysis using grand canonical Monte Carlo (GCMC) identified the presence of an unstable water molecule near the piperazine in the binding site. It was hypothesized that displacement of this water molecule would result in potency gains. This was achieved through either substitution of the piperazine near the quinazoline or the introduction of an additional tether to form the tetracycle. Further structure-activity relationship (SAR) analysis led to the replacement of the indazole for a fluorophenol to lower lipophilicity and improve clearance rates in human and rodent hepatocytes *in vitro*.

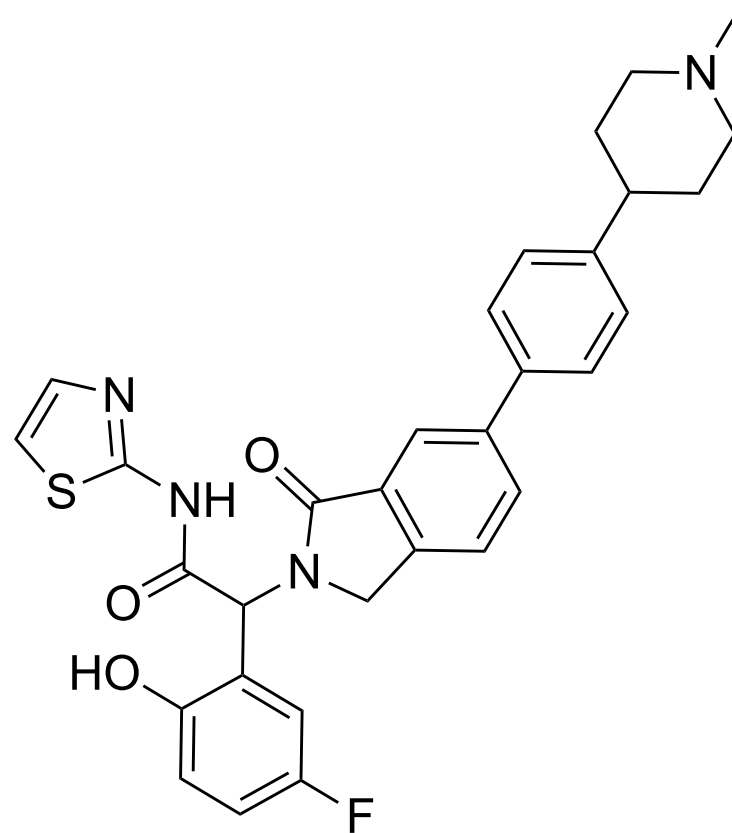
**Binding Mode.** The binding mode of AZD4625 (PDB: 7O70) and KRAS<sup>G12C</sup> highlights the quinazoline tethering strategy to direct the acrylamide terminal group to form a covalent bond with Cys-12 residue, and an H-bond with Lys-16 residue through the oxygen atom. This same interaction pattern is observed in the crystal structure of JDQ443 bound to KRAS<sup>G12C</sup>, although a different rigid spirocyclic linker strategy was employed.

**Preclinical Pharmacology.** *In vitro* cellular assays in KRAS<sup>G12C</sup> mutant vs non-KRAS<sup>G12C</sup> cell lines demonstrated a >100-fold potency reduction in non-KRAS<sup>G12C</sup> cell lines, indicating high selectivity of AZD4625. *In vivo* efficacy studies in KRAS<sup>G12C</sup> mutant MIA PaCa-2 xenograft mice were done at doses of 4 mg/kg, 20 mg/kg, and 100 mg/kg. Dose-dependent tumor regression was observed, with an associated dose-dependent decrease in the key RAS/MAPK signaling pathway gene DUSP6.

**Clinical Development.** No registered clinical trials for AZD4625 have been found as of May 20th, 2022, though a Ph. I trial is said to be pending.

# JBJ-09-063

## EGFR



allosteric mutant-EGFR inhibitor

in vivo efficacy in osimertinib-resistant xenograft models

from opt. of prev. disclosed EGFR inhibitor

Nat. Cancer

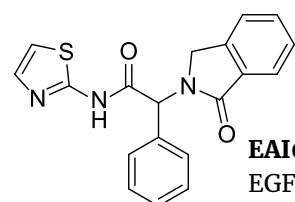
Dana-Farber Cancer Institute, Boston, MA

**Context.** JBJ-09-063 (Dana-Farber Cancer Institute) is an oral allosteric EGFR inhibitor currently in pre-clinical development for the treatment of EGFR L858R-mutant non-small cell lung cancer (NSCLC). Despite the availability of 3 generations of EGFR TKIs for the treatment of EGFR-mutant NSCLC, drug resistance and associated disease relapse are highly prevalent. There is room for improvement in this therapeutic area, even with third-generation agents, such as osimertinib, that have demonstrated superior clinical outcomes. In a space currently dominated by agents targeting EGFR's ATP-competitive site, JBJ-09-063 instead targets an allosteric site generated by the L858R mutation. Similar to other inhibitors currently being evaluated in preclinical studies, this binding strategy is at the center of a novel fourth generation of EGFR TKIs with the potential to overcome the poor mutant-selectivity of existing agents. Notably, the compound was designed to be effective as a single agent against EGFR<sup>L858R/T790M</sup> double and EGFR<sup>L858R/T790M/C797S</sup> triple mutation, which are resistant to all currently available EGFR TKIs, including osimertinib. Since JBJ-09-063 is able to co-bind with osimertinib, their co-administration in mutant cell lines potentiated tumor shrinkage and resulted in delayed tumor regrowth. A similar allosteric inhibitor, the sixth generation anti-Bcr-Abl agent asciminib was approved last year and was recently highlighted on our website. Despite these advantages, Dana-Farber researchers found that the efficacy of JBJ-09-063 was affected by homo or heterodimerization with other ErbB family members, an issue unique to allosteric inhibition of EGFR. This suggests a possible mechanism for resistance that may render the compound not so different from predecessor EGFR TKIs, which exhibit resistance via other mechanisms such as EGFR<sup>C797S</sup> mutation. No evidence is available yet on whether JBJ-09-063 is a CNS penetrant, which is a key clinically desirable property of osimertinib. It will be interesting to see how this molecule progresses during clinical development, which is yet to begin.

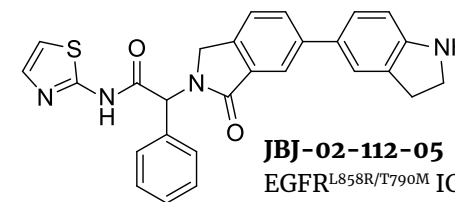
**Reviewer Comments.** Reviewer Callie Bryan says, "JBJ-09-063 provides a very subtle change over the previously reported JBJ-04-125-02, a piperazine to an N-methyl piperidine. Despite similar binding modes, JBJ-09-063 was significantly more potent with improved oral bioavailability. This yields comparable in vivo efficacy to osimertinib in a patient-derived DFCI52 xenograft model, and superior results in C797S models. Further development is still required for clinical success of an allosteric EGFR inhibitor, though."

**Mechanism of Action.** Unlike currently approved TKIs which target the ATP-competitive site of EGFR, JBJ-09-063 is an allosteric inhibitor that binds to a novel site in EGFR created by the L858R mutation. Allosteric binding of the compound precludes dimerization of EGFR, locking the receptor in the inactive state. Interestingly, EGFR dimerization antagonized binding of the allosteric inhibitor through the same mechanism. The researchers speculated that a threshold of EGFR expression exists below which baseline dimerization is minimal, and an allosteric inhibitor will be effective, but above which the inhibitor will lose efficacy. This reveals possible bypassing mechanisms for developing resistance that could be encountered with the use of these allosteric inhibitors in patients, a potentially important drawback given that ATP-competitive inhibitors are free of this limitation.

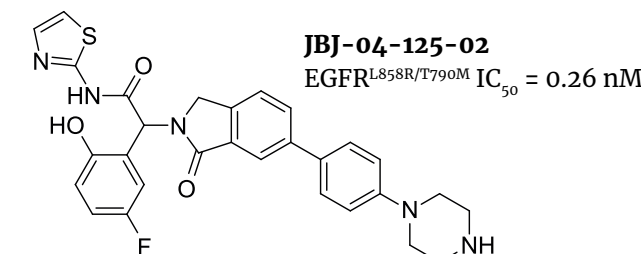
**Hit-Finding Strategy.** A thiazole amide allosteric inhibitor compound EAI001 was previously identified through a library screening of ~2.5 million compounds exhibiting special selectivity for EGFR<sup>L858R/T790M</sup> double and EGFR<sup>L858R/T790M/C797S</sup> triple mutation over wild-type EGFR. The incorporation of a 2-hydroxy-5-fluoro to the phenyl moiety led to a potency-enhanced analog EAI045 (EGFR<sup>T790M/L858R</sup> IC<sub>50</sub> = 3 nM). However, EAI045 was ineffective as a single agent due to the different potency in the EGFR dimer complex. Further optimization of EAI001 with the incorporation of a 5-indole substituent appended to the indolinone moiety led to the identification of JBJ-02-112-05. Improved potency was achieved by the incorporation of 2-hydroxy-5-fluorophenyl leading to the discovery of the JBJ-04-125-02 starting point.



EAI001  
EGFR<sup>L858R/T790M</sup> IC<sub>50</sub> = 24 nM



JBJ-02-112-05  
EGFR<sup>L858R/T790M</sup> IC<sub>50</sub> = 15 nM



JBJ-04-125-02  
EGFR<sup>L858R/T790M</sup> IC<sub>50</sub> = 0.26 nM

**Lead Optimization.** Allosteric inhibitors bind to a unique site formed as a result of the EGFR L858R mutation, distinct from the ATP site, and as such will not be impacted by most acquired EGFR mutations that can limit the efficacy of TKIs. The isoindolinone series compound JBJ-04-125-02 was modified with alterations at the phenyl ring to identify a more potent allosteric inhibitor. JBJ-09-063 contains a terminal N-methylpiperidine ring in place of a terminal piperazine ring in JBJ-04-125-02 highlighted in blue.

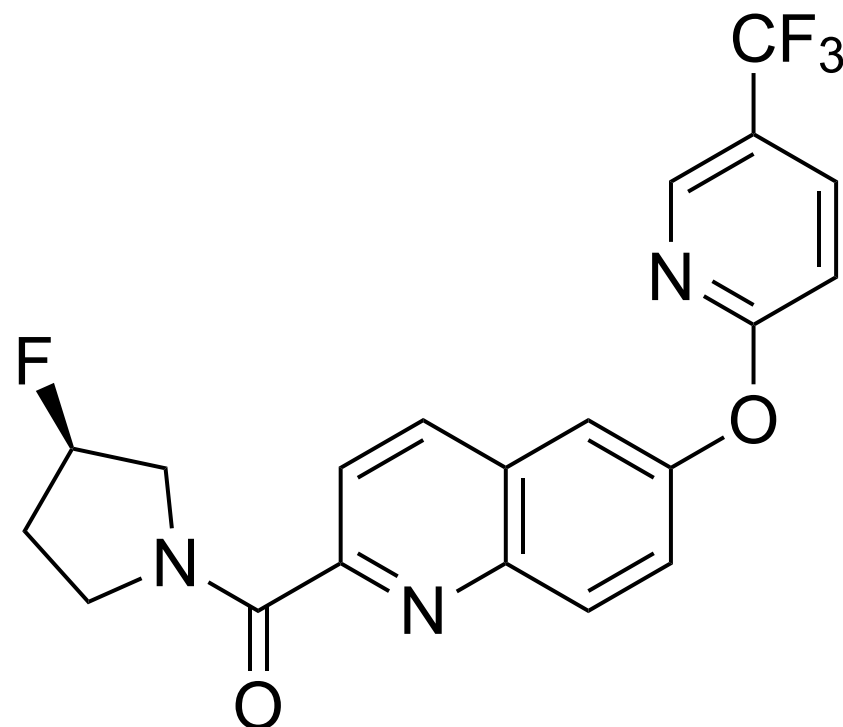
**Binding Mode.** Molecular modeling analysis revealed that secondary mutations in the ATP-binding site in C797S, L718Q, L792F, and G796S mutant EGFR led to steric clashes with osimertinib (PDB 4ZAU), limiting the covalent interaction. Since these mutations are local to the ATP site, they are not expected to affect the binding of allosteric inhibitors, including JBJ-09-063 (PDB 7JXQ). In triple mutant cell lines, JBJ-09-063 was more effective at inhibiting EGFR, Akt, and ERK1/2 phosphorylation than osimertinib.

**Preclinical Pharmacology.** Cell- and patient-derived xenograft mice harboring various EGFR mutations were used for the in vivo studies. In two models harboring the EGFR<sup>L858R/T790M</sup> mutation, a dose-dependent reduction in tumor volume was observed with JBJ-09-063, with the 50 mg/kg dose demonstrating comparable efficacy to osimertinib dosed at 25 mg/kg. After further engineering both models to harbor the EGFR<sup>L858R/T790M/C797S</sup> mutation, the animals were found to be resistant to osimertinib but sensitive to JBJ-09-063. Combining the compound with third-generation agent osimertinib or the first generation gefitinib which both bind in the ATP-competitive site, allowing for cooperative co-binding with JBJ-09-063, showed improved tumor shrinkage and delayed regrowth. Mutant selectivity of the compound was shown by its low activity in animals harboring EGFR-WT tumors, while it demonstrated strong activity in cells harboring the EGFR<sup>L858R</sup> mutation.

For more information on allosteric inhibitors of EGFR in development, see [US1117890B2/US10882848B2](#) (Roche), [US10450310B2](#) (allosteric PROTAC EGFR degrader, Dana Farber Cancer Institute, Inc.), [US20220112199A1](#) (Roche), [US20210346395A1/US20210040088A1](#) (Dana Farber Cancer Institute, Inc.), [US20210332029A1](#) (Korea Research Institute of Chemical Technology), [DDC-01-163](#), [DDC4002](#), [TREA-0236](#).

# ABBV-318

Na<sub>v</sub>1.7/1.8



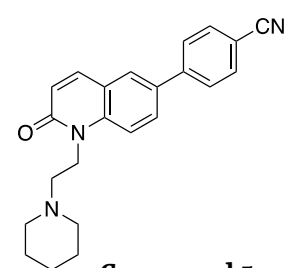
**Context.** [ABBV-318 \(AbbVie\) is a CNS-penetrating, oral inhibitor of Na<sub>v</sub>1.7/Na<sub>v</sub>1.8 being developed for pain treatment.](#) Despite being a highly validated pain target due to its important role in excitable cells, Na<sub>v</sub>1.7 inhibition has not lived up to its potential, and translation of the promising preclinical observations to human studies has been [elusive](#). A close isoform, Na<sub>v</sub>1.8, which has [mostly encountered similar fates](#) (e.g. [XEN-402](#)) in preclinical and clinical studies as Na<sub>v</sub>1.7, has recently entered the spotlight following a [Ph. II readout from Vertex that reported positive data for the Na<sub>v</sub>1.8 inhibitor VX-548](#) (structure undisclosed, but related to prodrug VX-150). Similar to Na<sub>v</sub>1.7, Na<sub>v</sub>1.8 has been implicated as a [key mediator of inflammatory pain](#), suggesting that a dual Nav1.7/Nav1.8 inhibitor may be a good clinical candidate due to the potential for stronger therapeutic action. For instance, one of the reasons cited for the lack of clinical success for Na<sub>v</sub>1.7 inhibitors is [strong selectivity](#): agents with high selectivity may result in overall less effective analgesia, while less selective agents may increase the analgesic effect, especially if combined with other targeting agents. Therefore, the CNS-penetrable ABBV-318, having dual Na<sub>v</sub>1.7/Na<sub>v</sub>1.8 activity, has the potential to succeed where many previous agents have failed. This would be ironic if true given the significant challenges over the years in identifying inhibitors selective for Na<sub>v</sub>1.7.

**Target.** [Na<sub>v</sub> channels](#) are key in excitable cells, making them attractive targets for pain therapeutics. Notably, the Na<sub>v</sub>1.7 and Na<sub>v</sub>1.8 isoforms which are highly expressed in nociceptors have undergone [extensive preclinical validation](#) as pain targets. [Gain-of-function mutations in Na<sub>v</sub>1.7 have been associated with inherited pain syndromes](#) while [loss-of-function mutations have been associated with pain insensitivity](#). Similarly, patients with chronic neurologic pain or hyperalgesia have been [shown](#) to express high levels of Na<sub>v</sub>1.8.

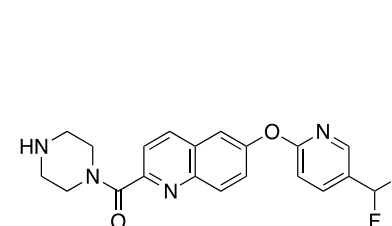
**Mechanism of Action.** Na<sub>v</sub> channel modulators are [either](#) pore blockers that physically occupy the channel pore or allosteric modulators that bind and lock the channel in a specific conformational state. ABBV-318 is a state-dependent Na<sub>v</sub>1.7 inhibitor that preferentially binds to the inactivated state of the channel, although data on the binding mode and specific interactions at the channel binding site have yet to be reported by AbbVie scientists.

**Hit-Finding Strategy.** “Compound 5” was identified through an electrophysiology-based high throughput screen presenting CNS penetrant features, good potency, and PK parameters.

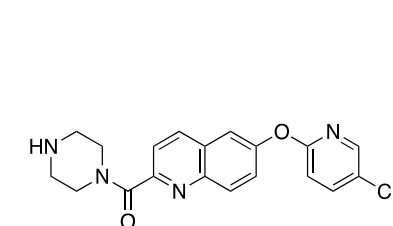
**Lead Optimization.** The structure-activity relationship (SAR) progression for optimization of the series focused on maintaining potency at Na<sub>v</sub>1.7, improving selectivity over the hERG channel, and overcoming the phospholipidosis (PLD) observed with the initial leads. While PLD is not considered a toxicological event, it should be avoided whenever possible. The introduction of moderately polar heteroaryl groups at the 6-position of the quinoline and removal of a basic amine at the 2-position culminated in the discovery of ABBV-318. Removing the basic amine proved most effective, resulting in compounds with consistently low clearance and good pharmacokinetic properties; it also allowed the series to overcome the challenge of phospholipidosis. A PLD score < 180 and a PLD index < 0.7 generally indicate a low probability of PLD induction.



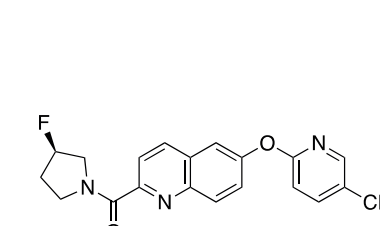
**Compound 5**  
(HTS hit)  
FRET hNa<sub>v</sub>1.7 IC<sub>50</sub> = 0.94 μM



**Compound 50**  
FRET hNa<sub>v</sub>1.7 IC<sub>50</sub> = 2.44 μM  
PLD Score (*in silico*) = 78  
PLD Index (*in vitro*) = 0.92



**Compound 51**  
FRET hNa<sub>v</sub>1.7 IC<sub>50</sub> = 0.92 μM  
PLD Score (*in silico*) = 198  
PLD Index (*in vitro*) = 0.735



**ABBV-318**  
FRET hNa<sub>v</sub>1.7 IC<sub>50</sub> = 2.8 μM  
PLD Score (*in silico*) = 198  
PLD Index (*in vitro*) = 0.735

**Preclinical Pharmacology.** Fluorescence resonance energy transfer (FRET)-based and electrophysiological assays were used to assess the efficacy and selectivity of ABBV-318 against other Na<sub>v</sub>1 channels. Importantly, the compound had little activity against the human Ether-`a-go-go-Related Gene (hERG) channel (IC<sub>50</sub> = 25.5 μM) which mediates cardiac physiology and Na<sub>v</sub>1.5 (IC<sub>50</sub> = 33 μM) which is [considered a cardiac liability channel](#). *In vivo* studies in a rat mono-iodoacetate-induced osteoarthritis ([MIA-OA](#)) [model of pain](#) demonstrated efficacy of the compound against Na<sub>v</sub>1.7 (IC<sub>50</sub> = 1-3 μM) as well as Na<sub>v</sub>1.8 (IC<sub>50</sub> = 4-6 μM), while efficacy was enhanced with sub-chronic dosing.

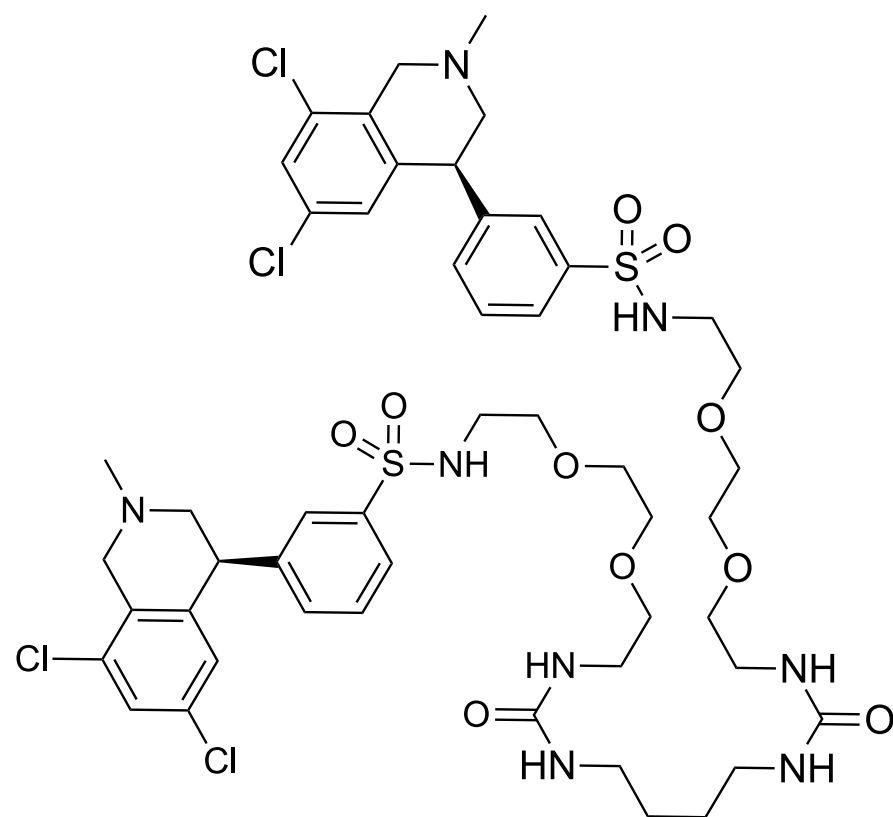
**Clinical Development.** ABBV-318 is preclinical, and the only disclosed selective Na<sub>v</sub>1.8 blocker remaining in clinical trials appears to be VX-548. Several Na<sub>v</sub>1.8 blockers have been discontinued: PF-04531083 (phase 2 - [NCT01512160](#) - discontinued), PF-06305591 (phase 1 - [NCT01776619](#) - discontinued), VX-128 (discontinued), VX-150 (phase 2 - [NCT03764072](#) - discontinued), and VX-961 (phase 1 discontinued).

oral CNS-penetrant Na<sub>v</sub>1.7/1.8 blocker  
in vivo efficacy in rodent pain models  
electrophysiology-based HTS and opt.  
*Bioorg. Med. Chem.*

AbbVie, North Chicago, IL

# tenapanor

## NHE3



oral gut-restricted Na<sup>+</sup>/H<sup>+</sup> exchanger inhibitor

FDA-approved IBS treatment

from literature starting point and opt

ACS Med. Chem. Lett.

Ardelyx Inc., Fremont, CA/Waltham, MA

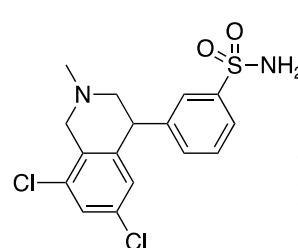
**Context.** Tenapanor (Ardelyx) is an oral, first-in-class Na<sup>+</sup>/H<sup>+</sup> exchanger isoform 3 (NHE3) inhibitor approved by the FDA for irritable bowel syndrome with constipation (IBS-C) in adults. NHE3 is expressed predominantly in the gut and kidney and its role as a key mediator of sodium and water homeostasis makes the protein an ideal target for multiple disease states such as hypertension, heart/kidney failure, diabetes mellitus, irritable bowel syndrome (IBS), constipation, and even hyperphosphatemia. However, this also presents a drug discovery challenge since systemic exposure could mean an undesired inhibition of renal NHE3. Therefore, critical to the development of tenapanor for IBS-C by Ardelyx scientists was the identification of an agent with potent Na<sup>+</sup>/H<sup>+</sup> antiport activity in the gut that exhibited poor bioavailability. Tenapanor is the first and only NHE3 inhibitor approved for this indication and represents the first novel mechanism for IBS-C since the approval of linaclotide (Linzess) in 2012. Although the drug was approved in 2019, its launch for IBS-C was only recently announced by Ardelyx. The company's plans to expand tenapanor's indication for hyperphosphatemia in chronic kidney disease faced a significant setback last year after the FDA issued a complete response letter citing the "small and unclear clinical significance" of the data, although the endpoints were met in a Ph. III trial evaluating the indication. A formal appeal by Ardelyx late last year was recently denied by the FDA. However, the agency has just recently agreed to convene an advisory committee to consider the application, in what may be Ardelyx's final chance to make an entry into the lucrative kidney drug market where \$800M in potential sales within 5 years awaits.

**Target.** NHE3, a membrane-associated protein expressed on the brush border membrane of renal and intestinal epithelial cells, mediates the absorption of sodium ions. The protein has been shown to play a key role in transepithelial Na<sup>+</sup> absorption compared to other Na<sup>+</sup>/H<sup>+</sup> exchangers, while NHE3-deficient mice have been associated with spontaneous distal colitis.

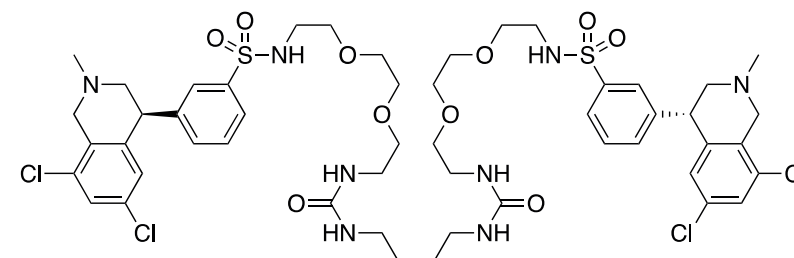
**Mechanism of Action.** The tenapanor program was the fruit of an AZD/Ardelix collaboration. The compound inhibits NHE3 on the apical surface of enterocytes, restricting sodium reabsorption in the gut which increases water secretion. Overall, this inhibitory action speeds up the bowel transit time, softening stool consistency and increasing stool frequency. Ardelyx also reported data from animal studies that revealed that the drug mitigates abdominal pain caused by IBS-C by inhibiting TRPV-1-dependent signaling. Specifically, treatment with tenapanor decreased visceral hypersensitivity and normalized sensory neuronal excitability and TRPV-1 currents in the colon.

**Hit-Finding Strategy.** Ardelyx scientists scanned the literature to find possible pharmacophores with reported NHE3 inhibitory activity. Compounds were tested in a deacidification assay to determine their ability to inhibit Na<sup>+</sup>/H<sup>+</sup> exchange, using a pH-sensitive dye. The most promising compound, a phenyl-tetrahydroisoquinoline disclosed in a Sanofi patent (US6911453B2), was selected for further optimization, with the main goal being the blockage of sodium absorption in the gastrointestinal tract, without exposure to the kidney. An initial screen identified compound 1, with 98% oral bioavailability in rats.

**Lead Optimization.** Hit optimization was focused on probing regions on "compound 1" tolerant to chemical modification and determining where the activity could be improved. Stereochemistry, sulfonamide regiochemistry, linker length, and core motifs were modified to culminate in a potent and minimally absorbed chemotype suitable for clinical development.



**Compound 1**  
pIC<sub>50</sub> = 6.2  
98% bioavailable



**Tenapanor**  
pIC<sub>50</sub> = 9.3  
<1% bioavailable

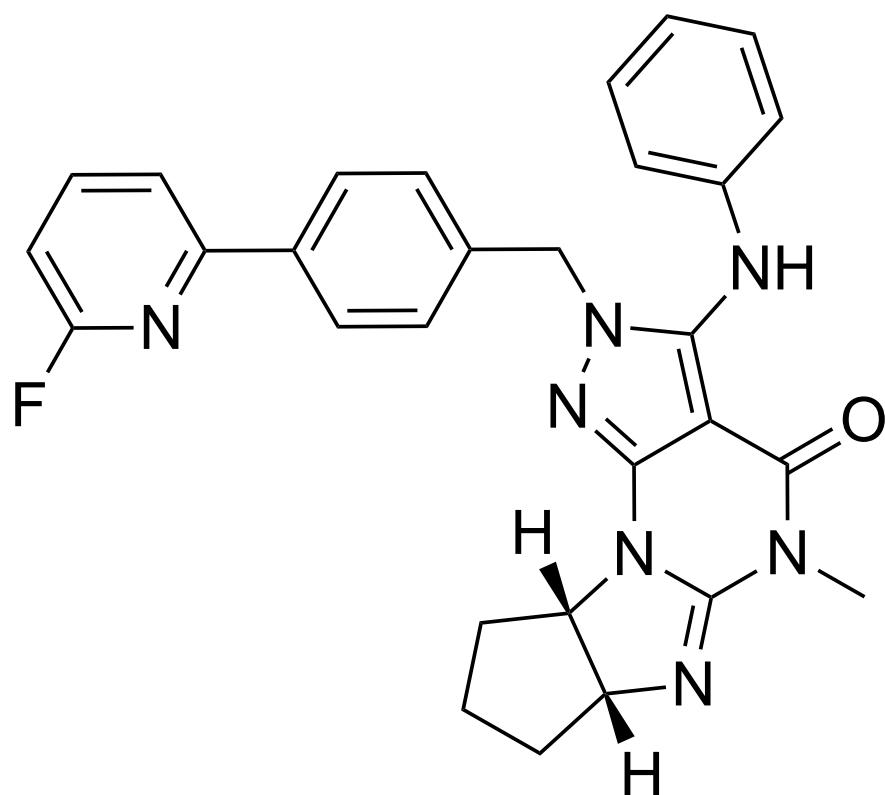
**Binding Mode.** The S-configuration was strongly preferred, suggesting a synergistic binding mode for the dimeric pharmacophore. The on-target inhibition of NHE3 causes a decrease in the intracellular pH (pH<sub>i</sub>) of intestinal epithelial cells. This decrease in pH<sub>i</sub> is thought to modulate the tight junctions between the epithelial cells, resulting in an increase in the transepithelial electrical resistance that restricts the paracellular permeability of phosphate, the major pathway for intestinal phosphate absorption.

**Preclinical Pharmacology.** A cell-based rat/human NHE3 inhibition assay was used to evaluate rat/human NHE3-mediated Na<sup>+</sup>/H<sup>+</sup> antiport activity of the compound observed pIC<sub>50</sub>s of 9.3 and 7.8 for human and rat NHE3 proteins, respectively. This method was based on a previously described pH recovery assay. In animal studies using Sprague Dawley rats known to express NHE3, tenapanor increased stool water content in a dose-dependent manner, while a high drug recovery rate (92%) was observed. Furthermore, the drug decreased urine Na<sup>+</sup> excretion in a dose-dependent manner, at 0.1, 0.3, and 1.0 mg/kg.

**Clinical Development.** Tenapanor's clinical efficacy in constipation-predominant irritable bowel syndrome was evaluated in three main clinical trials efficacy studies (NCT02686138, NCT02621892, NCT01923428). Clinical trial results showed that tenapanor has minimal systemic absorption in humans at a dose of 50 mg PO BID, leading to a significant improvement in irritable bowel syndrome with symptoms of constipation. Tenapanor was approved by the U.S. Food and Drug Administration (FDA) in 2019, for the treatment of irritable bowel syndrome with constipation in adults. During clinical development, it was observed that tenapanor lowered serum phosphorus levels in dialysis patients with hyperphosphatemia, a major comorbidity in this patient population, by preventing the intestinal absorption of phosphate. Although the results of the clinical trials point to a significant reduction in the serum phosphate levels in patients with hyperphosphatemia receiving maintenance hemodialysis, the FDA rejected the approval (claiming small and of unclear clinical significance) for this application asking for additional trials.

# lenrispodun (ITI-214)

PDE1



oral, CNS-penetrant, picomolar PDE1 inhibitor

Ph. I/II in neurology and heart failure

from literature starting point, LBDD and SBDD

Neuropsychopharmacology

Intra-Cellular Therapies, New York, NY

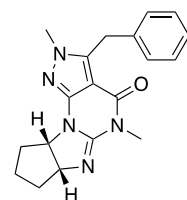
**Context.** **Lenrispodun (Intra-Cellular Therapies)** is a phosphodiesterase (PDE) type 1 (PDE1) inhibitor being developed for CNS and non-CNS disorders, including heart failure, and cancer. Studies to identify PDE inhibitors date back at least 30 years, and at **least 10 drugs have been approved** targeting other PDE proteins (spearheaded by the PDE5 inhibitor **sildenafil [Viagra]**). However, no PDE1 inhibitors have been approved for at least two decades, despite the existence of the classic PDE1 inhibitor **vinpocetine (structure)**, and **reports** of other PDE1-targeting agents during this time. This may be attributable to the general complexity of PDE proteins, as well as the high structural similarity among over 100 isoforms which may hinder selectivity, a challenge Intra-Cellular Therapies scientists are determined to overcome. Key to the development of lenrispodun was the identification of agents highly selective for PDE1, but with minimal activity against other family members, such as **PDE6 that has been implicated in vision**. With its **ongoing evaluation in Ph. I studies** for Parkinson's and heart failure, lenrispodun may currently be the most advanced PDE1 inhibitor, considering that **clinical trials involving vinpocetine over the years have not yielded promising data**. Interestingly, **early preclinical data** also suggest the drug may have antitumor activity.

**Target.** **PDEs**, comprising a large and complex superfamily of 11 main members characterized by 21 genes that encode more than 100 proteins, mediate the hydrolysis of cAMP and cGMP throughout the body, including the brain. Of the 11 family members, PDE1 and four others (PDE2, PDE3, PDE10, PDE11) act on both cAMP and cGMP with varying affinities. Despite the apparent functional redundancies, PDE proteins are key players in specific physiological processes, and inhibition of these proteins has been **shown to prolong and amplify cAMP/cGMP signaling**. Probing of PDEs with small molecule inhibitors in animal models has revealed an **improvement in cognitive performance, enhancement of object memory**, and even **reduction in mechanical hyperalgesia**.

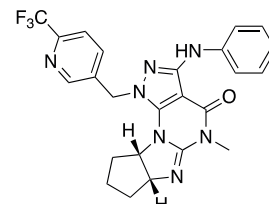
**Mechanism of Action.** Cyclic nucleotide substrates **make specific interactions** at the PDE catalytic site, including the formation of a key hydrogen bond at a conserved active-site glutamine and a hydrophobic clamp that surrounds the purine ring of these substrates. Overall, PDE1 inhibition enhances the levels of cAMP/cGMP in cells, but the subsequent downstream effects depend on the body system involved. **In the CNS**, this increases the expression of neuronal plasticity-related genes, neurotrophic factors, and neuroprotective molecules. In the cardiovascular system, one study found that inhibition of the protein sanctions the stimulation of cardiomyocyte contraction by the Ca<sub>v</sub>1.2 channel, while **another observed** the induction of vasodilation with a concomitant reduction in blood pressure. Intra-Cellular Therapies scientists have also **published two additional reports** detailing the role of PDE1 inhibition in **reducing age-related elevated vasoconstriction** as well as **normalization of vasodilator function in progressive vascular smooth muscle dysfunction**. At the 2021 AACR annual meeting, Intra-Cellular Therapies presented data on the role of PDE1 in the immune system, suggesting that the protein acts to reduce macrophage and microglial activity, which may make lenrispodun a potential antitumor agent also.

**Hit-Finding Strategy.** Analysis of published PDE inhibitors indicated that **the pyrazolo[3,4-d]pyrimidine derivatives first reported in 1997 by Schering-Plough researchers could** be a good starting point, as they showed nanomolar to micromolar activity as dual PDE1 and PDE5 inhibitors; for instance, compound 4b, showed a PDE1 IC<sub>50</sub> of 55 nM. In 2016, **Intra-Cellular Therapies took the chance to develop this fused ring as a potential phosphodiesterase 1 for the treatment of cognitive impairment associated with neurodegenerative and neuropsychiatric diseases**.

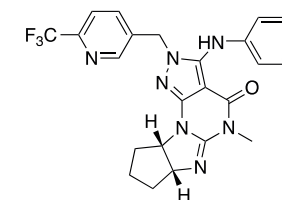
**Lead Optimization.** Using a combination of ligand-based and structure-based drug design, and starting from compound 4b, SAR strategies focused on modifying different regions of the basic scaffold. The most promising modifications were found through substitution of the C3-toluidyl group and the N2-methyl group in 4c, which ultimately enhanced binding affinity to PDE1 over 24,000 times more than the unsubstituted analogs. Analysis of the binding mode of phosphodiesterase enzymes with cGMP indicated a key H-bond between the purine nitrogen 7 and an adjacent amino acid residue in the catalytic site. Aiming to incorporate this binding mode in the initial scaffold, the ICT scientists introduced an amino group at position 3 of the pyrazolopyrimidine system. Interesting SAR was observed when comparing N1- vs. N2- isomers, with compound 36 showing 22 times more binding affinity for PDE1 than the unsubstituted isomer, and compound 37 showing a 730-fold increase. Further optimization led to the discovery of **ITI-214 (Lenrispodun)**; which is a picomolar PDE1 inhibitor (K<sub>i</sub> = 0.058 nM) with excellent selectivity against other PDE family members and against a panel of enzymes, receptors, transporters, and ion channels.



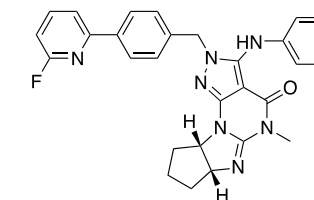
**Compound 4b**  
IC<sub>50</sub> = 55 nM



**Compound 36**  
K<sub>i</sub> = 0.065 nM (PDE1)  
K<sub>i</sub> = 0.70 nM (PDE4)



**Compound 37**  
K<sub>i</sub> = 0.0019 nM (PDE1)  
K<sub>i</sub> = 1.2 nM (PDE4)



**Lenrispodun (ITI-214)**  
K<sub>i</sub> = 0.000058 nM (PDE1)  
K<sub>i</sub> = 0.16 nM (PDE4)

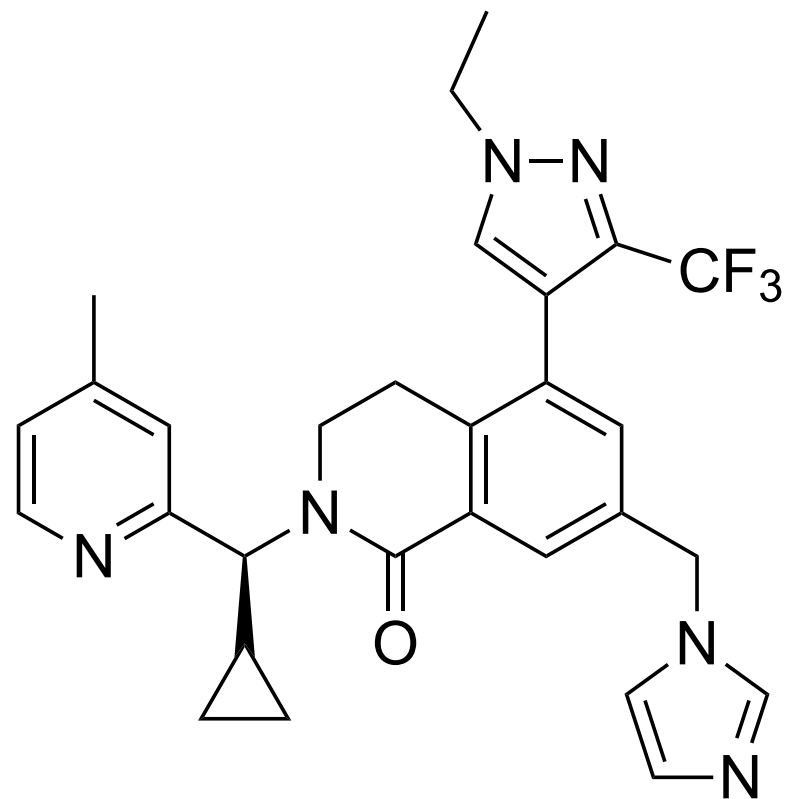
**Binding Mode.** The crystal structure of the catalytic domain of human recombinant PDE1B enzyme complexed with **ITI-214** (PDB code: **5B25**) revealed the phenylamino group attached to the pyrazole carbon is buried deeply in a hydrophobic subpocket formed primarily by F392, L388, M389, V417, S420, T385, and L409. The cyclopentyl group fused with a stereochemistry of (6aR,9aS) bends down and fits nicely into the catalytic pocket and has van der Waals interactions with M336 and several other residues. The phenylene and pyridyl groups of the 4-(6-fluoropyridin-2-yl)benzyl side chain of 3 each had  $\pi$ - $\pi$  interactions with F424 and F427, respectively, in addition to various van der Waals interactions with other residues such as G423, S420, F340, and I428. A water-mediated zinc-nitrogen interaction was also observed. Another interesting feature is the conserved strong 3-amino H-bonding interaction with N421 residue shown in the hit compound.

**Preclinical Pharmacology.** *In vitro* selectivity studies included **evaluation** of the phosphodiesterase inhibitory activity of the drug against various recombinant isoforms of PDE1 and PDE2-11 as well as assessment of off-target binding to 70 key receptors, enzymes, and channels. Potent inhibition of PDE1A (K<sub>i</sub> = 33 pmol) and high selectivity vs. other PDE isoforms (1000-fold) were observed. The drug also demonstrated minimal off-target binding. *In vivo* behavioral studies were done using Wistar rats. Memory performance was assessed using the **novel object recognition test**, while **conditional avoidance responding** was also evaluated. Animals treated with the drug had improved memory performance characterized by memory acquisition, consolidation, and retrieval. The drug also had no effect on the pharmacokinetic profile of the antipsychotic risperidone.

**Clinical Development.** Lenrispodun completed Ph. I/II clinical trials (**NCT03489772** and **NCT03387215**) with 26 healthy individuals. Patients received, in random order, a single oral dose of placebo, lenrispodun 1.0 mg or lenrispodun 10.0 mg, and completed several tasks in the fMRI scanner, including the stop signal (n=24) and fear conditioning/extinction tasks (n= 22). Results provide evidence that 1.0 mg lenrispodun selectively improved neural inhibitory control without altering fear extinction processing. Currently, there are no selective PDE1 inhibitor trials listed as active in the clinicaltrials.gov registry. Few selective preclinical PDE1 inhibitors have been disclosed in the literature. Most of them also show inhibitory activity to other PDE enzymes. Some preclinical selective PDE1 inhibitors: SCH-51866 (PDE1/PDE 5 inhibitor), **PF-04822163** (PDE1B inhibitor - IC<sub>50</sub> 4.5 nM), **PF04471141** (PDE1B inhibitor - IC<sub>50</sub> 35 nM), **PF04677490** (PDE1B inhibitor - IC<sub>50</sub> 21 nM), **DNS-0056** (PDE1B inhibitor - IC<sub>50</sub> 26 nM)

# compound 41

## WDR5



oral WDR5 inhibitor

pM  $K_i$ , nanomolar in cells

from FBDD, SBDD, and PK opt.

*J. Med. Chem.*

Vanderbilt University School of Medicine,  
Nashville, TN

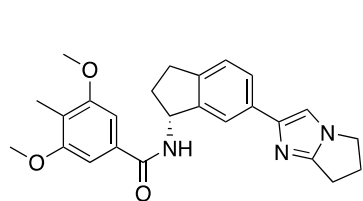
**Context.** “Compound 41” (Vanderbilt University School of Medicine) is an oral WD40 Repeat Domain 5 (WDR5) inhibitor being developed for various human cancers. The well-established role of epigenetic abnormalities in cancer development and progression has led to extensive studies to identify various epigenetic cancer inhibitors. Currently, seven such drugs have been approved by the FDA for diverse malignancies, and they target three major epigenetic drug targets: DNA methyltransferases (DNMTs), histone deacetylases (HDACs), and enhancer of zeste homolog 2 (EZH2). As a key mediator of multiple epigenetic regulatory complexes, WDR5 is emerging as an ideal epigenetic cancer target. Preclinical studies suggest that “compound 14” selectively targets cells with the mixed lineage leukemia (MLL) epigenetic signature through a potentially novel mechanism. *In vitro* efficacy and early *in vivo* pharmacokinetics data for the compound are promising and it will be interesting to see how this potential first-in-class drug progresses further.

**Target.** WD40 repeat domain proteins, one of the largest human protein families, act as scaffolds for protein interaction in multiprotein complexes, and are involved in multiple cellular networks. WDR5 is involved in several cellular processes and acts predominantly within the nucleus. One of the protein’s well-researched roles is its involvement in the activity of MLL1 histone methyltransferase complexes. The suitability of WDR5 as an oncology target emanates from the protein’s key role as a cofactor for the MYC family of oncoprotein transcription factors. Overexpression of the protein has been documented in several cancer types, while an *in vivo* model harboring a MYC mutant with limited binding to WDR5 demonstrated poor tumor progression due to impaired binding of MYC to chromatin.

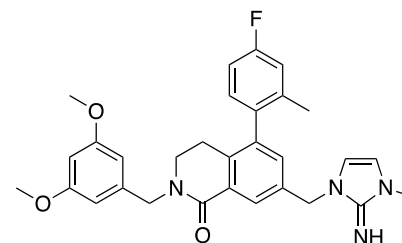
**Mechanism of Action.** An arginine-binding region in WDR5 dubbed the “WIN” site has been considered the target of inhibitors of the protein. Binding to this cavity has been suggested to selectively kill tumors harboring the MLL epigenetic signature. Due to WDR5’s key role in MLL-mediated histone methylation, it is thought that inhibitors targeting the WIN site inhibit MLL-rearranged cancer cells through changes in histone methylation. However, in a study, Vanderbilt scientists studying “compound 41” found that its killing of MLL-rearranged cancer cells was instead due to displacement of WDR5 from chromatin on genes responsible for protein synthesis.

**Hit-Finding Strategy.** Researchers from Vanderbilt University reported a WDR5 inhibitor series discovery through a fragment-based and structure-based medicinal chemistry campaign, with “compound 6e” reported as the most potent. The starting point for hit identification was a recombinant,  $^{15}\text{N}$ -labeled WDR5 (residues 22–334), used to screen a fragment library (>13,800 compounds) by recording SOFAST  $^1\text{H}$ - $^{15}\text{N}$  HMQC spectra of WDR5. Subsequent structure-based design was used to optimize these hits and resulted in the identification of non-peptidic small molecules derived from pyrrolo[1,2-*a*]imidazoles and dihydroisoquinolinone bicyclic cores as WDR5-WIN-site inhibitors, ultimately leading to the discovery of a potent WDR5 inhibitor with conformationally rigid 3,4-dihydroisoquinolin-1(2H)-one core and picomolar binding affinity (compound 1).

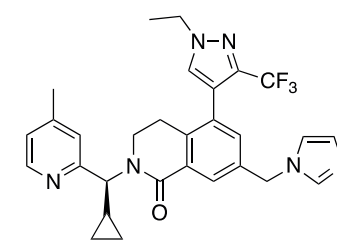
**Lead Optimization.** The use of an X-ray structure-guided pharmacophore-based convergent strategy to improve its druglike properties and pharmacokinetic profile, resulted in the discovery of “compound 41”. The dihydroisoquinolinone bicyclic core was modified at three different sites. Pyridine bearing an (*S*)-cyclopropyl, trifluoromethylpyrazole, and imidazole groups were successfully replaced in the hit compound 1; all modifications improved potency, solubility, pharmacokinetics, and oral bioavailability. The (*S*)-cyclopropyl group significantly improved the PK profile including *in vivo* clearance and oral exposure and maintained potent *in vitro* on-target potency.



**Compound 6e**  
 $GI_{50}$  = 7.25  $\mu\text{M}$  (MV4:11)  
 $K_i$  = 0.902 nM (WDR5)



**Compound 1**  
 $GI_{50}$  = 0.038  $\mu\text{M}$  (MV4:11)  
 $K_i$  < 0.02 nM (WDR5)



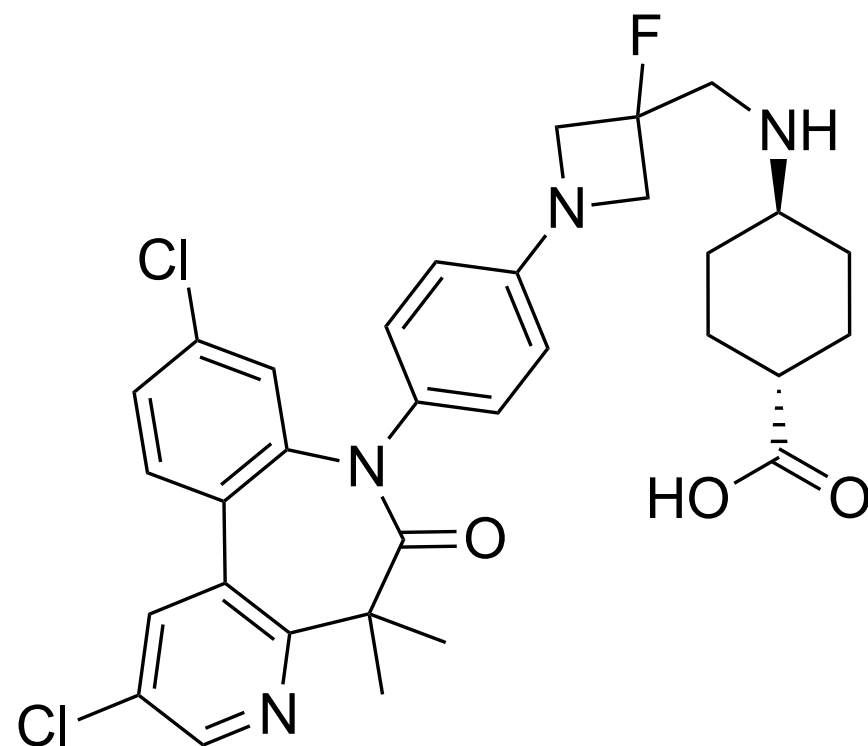
**Compound 41**  
 $GI_{50}$  = 0.013  $\mu\text{M}$  (MV4:11)  
 $K_i$  < 0.02 nM (WDR5)

**Binding Mode.** The X-ray structure (PDB ID: 7U9Y) confirmed that the 2-methyl imidazole moiety maintained critical binding interactions in the S2 subsite, which were critical to preserving the original binding mode to the WDR5 WIN site. 2-methyl imidazole maintains strong sandwiched  $\pi$ - $\pi$  stacking interactions with F133 and F263. The 4-methyl-2-pyridylmethyl group optimized interaction in the S7 subsite. The (*S*)-cyclopropyl group pointed out of the binding interface.

**Preclinical Pharmacology.** The compound demonstrated strong potency ( $K_i$  = <0.02 nM) in TR-FRET assays and nanomolar activity in cell proliferation assays involving the WDR5 sensitive MV4-11 ( $GI_{50}$  = 13 nM) and MOLM-13 (27 nM) cell lines, while it also showed selectivity in reference to the WDR5 insensitive K562 cell line (>200-fold). Overall, the pharmacokinetic profile of the compound was found to be desirable, although *in vivo* efficacy data have yet to be reported by Vanderbilt scientists.

# DS69910557

## hPTH1R



oral hPTH1R GPCR antagonist  
calcium-lowering activity in rodent  
scaffold-hopping from lit. starting point

*Bioorg. Med. Chem.*

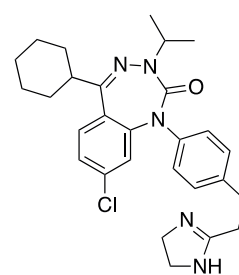
Daiichi Sankyo, Tokyo, JP

**Context.** [DS69910557 \(Daiichi Sankyo\)](#) is an oral inhibitor of parathyroid hormone (PTH) type 1 receptor (PTH1R) being developed as a calcium-lowering drug. The well-characterized secretin class receptor PTH1R is a principal regulator of bone remodeling and calcium ion homeostasis which makes it an attractive target for some endocrinopathies and bone disorders. The first report of a [PTH receptor inhibitor, BIM-44002](#), which showed preclinical efficacy, was in 1997, although the compound did not demonstrate calcium-lowering activity in human studies. Since then, at least three other small molecule PTH1R antagonists have been reported, including a [1,3,4-benzotriazepine-based lead, SW106](#), and [DS08210767](#), as well as the peptide antagonist [DPC-AJ1951](#). Additionally, at least three small molecule agonists of the receptor have been reported, including [AH-3960](#), [CH5447240](#), and [PCO371](#). Despite some promising preclinical data generated by some of these agents, none have advanced to clinical development. It remains to be seen whether DS69910557 will succeed where many of its predecessors seem to have failed.

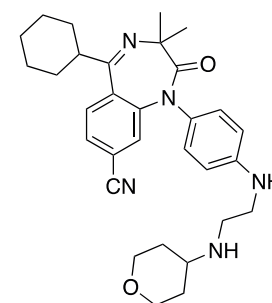
**Target.** [PTH1R](#) is a class B family G-protein-coupled receptor (GPCR) expressed predominantly in human bone and kidney tissues. It mediates PTH-dependent processes such as skeletal development, bone turnover, and mineral ion homeostasis. PTH1R as a drug target has been [well-validated](#). In [genetic studies](#), mutations in the protein have been associated with chondrodysplasia and other bone-related disorders, while hyperactive PTH1R [has been linked](#) with hyperparathyroidism. In a clinical [study](#) involving more than 1500 postmenopausal women with osteoporosis, treatment with PTH increased bone mineral density and fracture risk.

**Mechanism of Action.** PTH, secreted in response to low blood calcium levels, binds PTH1R and elicits different downstream effects depending on the tissue involved. In the kidney, this leads to stimulation of tubular calcium reabsorption through the effect of  $1\alpha$ -hydroxylase. In the bone, stimulation of PTH1R either directly or indirectly in osteoclasts stimulates the release of calcium from the matrix as well as modulates the synthesis/activity of downstream proteins such as osteoclast-differentiating factors. Therefore, inhibition of PTH1R is expected to impact these processes, although the specific mechanisms underlying the compound's action are yet to be reported by Daiichi Sankyo scientists.

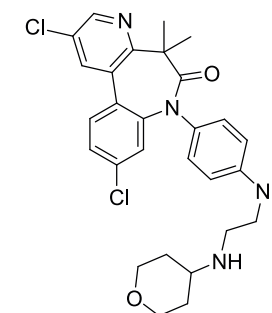
**Hit-Finding Strategy.** The starting point was 3,4-benzotriazepine-based compounds described in the patent application from the James Black Foundation (JBF). "[Compound 5](#)" was found to have antagonist activity at micromolar concentrations against PTH1R ( $IC_{50} = 9.4 \mu M$ ).



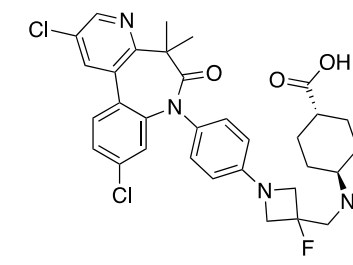
**Compound 5**  
 $IC_{50} = 9.4 \mu M$



**Compound 23**  
 $IC_{50} = 0.09 \mu M$



**DS37571084**  
 $IC_{50} = 0.17 \mu M$



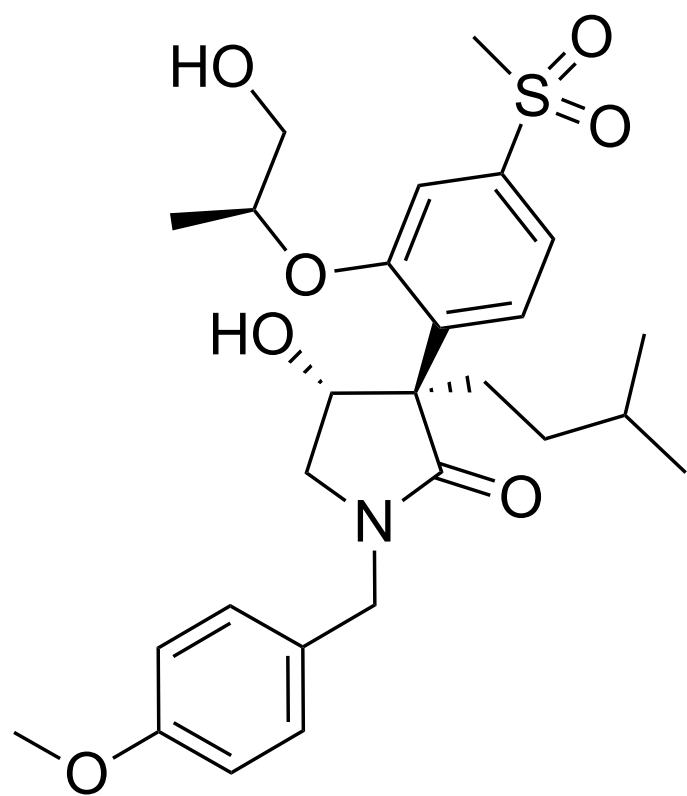
**DS69910557**  
 $IC_{50} = 0.08 \mu M$

**Lead Optimization.** From "compound 5", application of a scaffold-hopping approach identified "[compound 23](#)." However, this compound was not stable under acidic conditions due to the imine moiety. Successive optimization of the lead compound improved aqueous solubility, metabolic stability, and animal pharmacokinetics, culminating in the identification of [DS37571084 \(12\)](#). Finally, the introduction of the azetidinyll group bearing a cyclohexane-1-carboxylic acid led to compound [DS69910557 \( \$IC\_{50} = 0.08 \mu M\$ \)](#). Interestingly, the introduction of one fluorine group on the azetidine ring had a dramatic impact on PK profile in preclinical species, and compound 19e demonstrated high plasma exposure.

**Preclinical Pharmacology.** Oral administration of the compound at 10 mg/kg in Sprague Dawley rats resulted in a significant lowering of plasma calcium concentration at 3 and 8 hours vs. control ( $P < 0.05$ ). Additional preclinical data on the efficacy of the compound have yet to be reported.

# compound 14

## HIV-1 protease



potent HIV-1 protease inhibitor  
in vitro activity ( $IC_{50} = 0.0071 \mu\text{M}$ ,  $EC_{50} = 0.86 \mu\text{M}$ )  
from “pocket-to-lead” virtual screen and SBDD

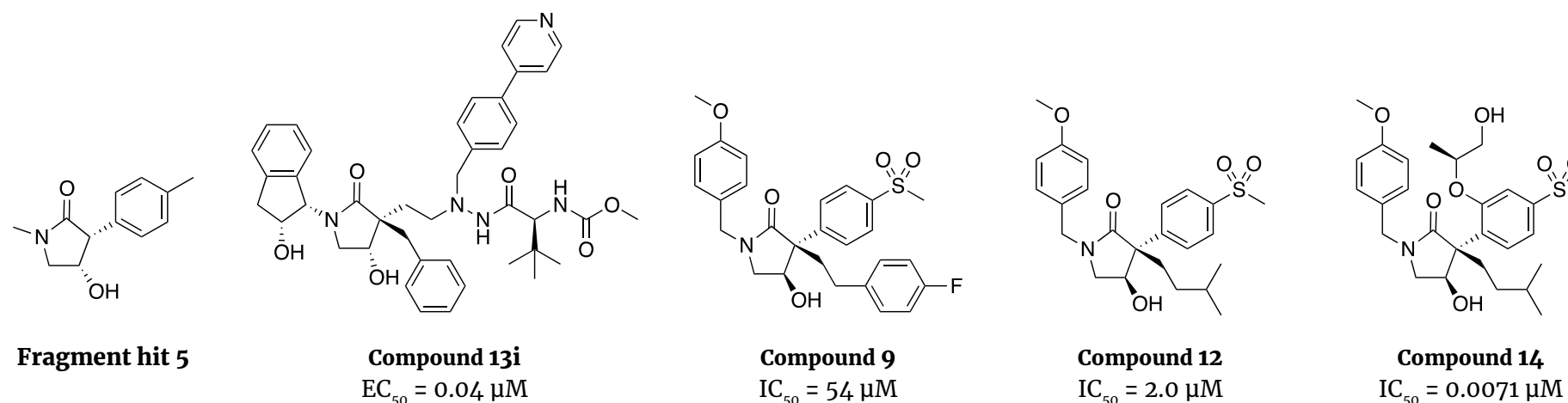
*J. Med. Chem.*

Shionogi, Osaka, JP

**Context.** “Compound 14” (Shionogi) is an HIV-1 protease inhibitor being developed for HIV treatment. Despite the existence of [two generations and a total of nine approved agents](#) targeting the [well-validated](#) HIV-1 protease, issues with [drug resistance](#) and [toxicity](#) still persist, highlighting the need for novel agents with unique mechanisms of action. BMS scientists adopted a novel “Pocket-to-Lead” strategy utilizing HIV-1 as the target to identify and optimize “**compound 14**” which exhibited promising in vitro efficacy and could provide a useful tool to further develop novel inhibitors targeting the protein.

**Hit-Finding Strategy.** A novel strategy named “Pocket-to-Lead” employed docking and *de novo* design. This strategy was applied to the Shionogi Virtual Library (SVL). As a result of the virtual screening, a conformationally constrained lactam moiety was identified. Searching this fragment within the literature was found a series of lactam-based PIs such as [“compound 13i”](#), [published by Wu, et al.](#) An extensive *de novo* design cycle (design-docking cycle) was carried out and identified the initial synthetic molecule “**compound 9**” that showed very weak activity,  $IC_{50}$  of  $54 \mu\text{M}$ .

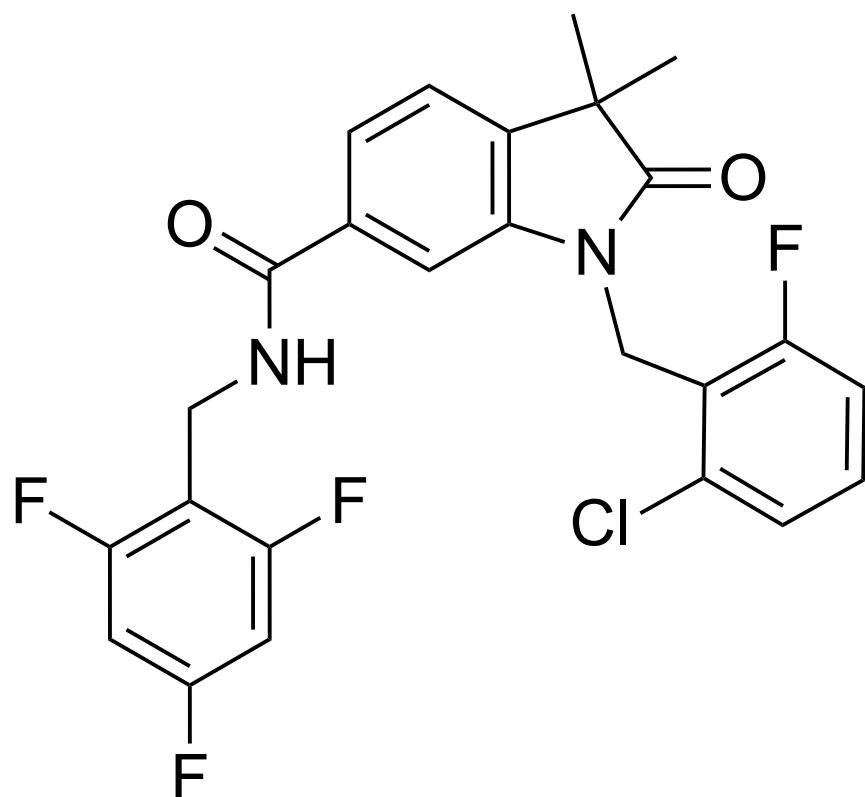
**Lead Optimization.** Given the promise of “**compound 9**”, the Shionogi scientists solved its X-ray structure bound to HIV-1 protease, followed by a grid inhomogeneous solvation theory (GIST) analysis. This analysis suggested that further modification of the hydrophobic ligands within the S1 and S1’ subsites may improve activity. Optimization of the S1’ ligand delivered “**compound 12**”, which showed a 30-fold increase in activity compared with “**compound 9**”. Subsequent optimization of the S1 ligand, lacking in “**compound 9**”, through the preparation and screening of a virtual library, indicated that an isopropoxy substitution *meta* to the sulfonyl group would best fill the S1 subsite. Furthermore, the addition of a hydroxyl to one of the terminal methyl groups of the isopropyl moiety allowed for direct interaction with the NH of Ile50, leading to “**compound 14**” ( $IC_{50} = 0.0071 \mu\text{M}$ ,  $EC_{50} = 0.86 \mu\text{M}$ ), and an improvement in the activity by approximately 10,000-fold, compared to “**compound 9**”.



**Binding Mode.** The X-ray crystal [structure of “compound 14” complexed](#) with HIV-1 protease ([PDB ID: 7WBS](#)) showed that the hydroxyl group of “compound 14” picked up a direct interaction with the NH of Ile50 in the flap. The methyl group of “**compound 14**” forms a van der Waals interaction with Leu 23’, Val82’, and Ile 84’. In addition to the interactions, the branched structure should contribute to the stabilization of the binding conformation of the side chain.

# compound 53

## STING



non-nucleotide STING agonist

novel mechanism for STING activation

from micromolar HTS hit

Nature

University of Texas Southwestern  
Medica Center, Dallas, TX

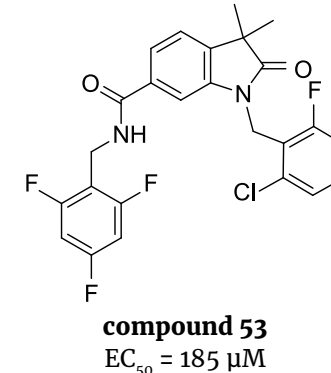
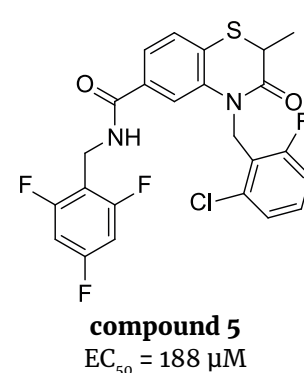
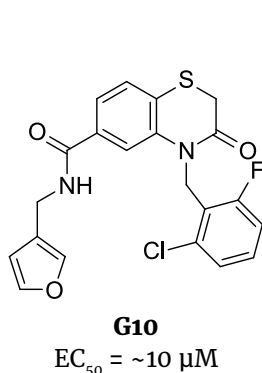
**Context.** [“Compound 53” \(University of Texas Southwestern Medical Center\) is a stimulator of interferon \(IFN\) genes \(STING\) agonist.](#) STING agonists have been heavily pursued in cancer immunology as [increasing data](#) suggests that the efficacy of immunotherapy can be enhanced by proteins such as STING that can induce a strong innate immune response through [regulation of type I interferon signaling](#). We have previously highlighted several STING agonists, including [Merck’s MK-1454 \(ulevostinag\)](#), which is currently the most advanced STING agonist and in Ph. II studies, [Aduro’s ADU-S100](#) which was terminated at Ph. II studies due to poor efficacy, and [Eisai’s E7766](#). “Compound 53” targets a unique pocket in the protein that allows for a potentiated effect since endogenous cGAMP is also able to bind simultaneously. If the novel mechanism of agonism confers a more potent immunostimulatory local effect in tumors, it may offer a path to different pharmacological profiles to address toxicity from systemic STING activation.

**Target.** The 2',3'-cyclic guanosine monophosphate-adenosine monophosphate (cGAMP) synthase (cGAS)-STING pathway acts as a principal sensor of cytosolic cyclic dinucleotides, ultimately leading to the expression of type I interferon. The ability of the pathway to induce the innate immune response, coupled with the potential for STING proteins to act as a bridge connecting innate and adaptive immunity, make the pathway an attractive target for autoimmune and oncology diseases alike. This target has been [well-characterized and heavily validated preclinically](#), with an extensive list of agents currently being pursued for several indications. Efficacy data has so far been disappointing though, likely in part due to the need for intratumoral delivery to avoid systemic immune activation (e.g. cytokine storm).

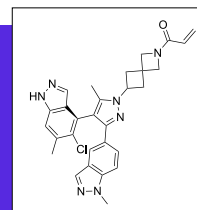
**Mechanism of Action.** Once induced by an upstream stimulus, cGAMP synthesized by cGAS binds to the endoplasmic reticulum-transmembrane adaptor protein STING, leading to a conformational change in the ligand-binding domain. This leads to oligomerization of the protein and subsequent translocation to the perinuclear compartment, which ultimately results in the transcription of innate immunity genes. [Structural and functional characterization data on the pathway have been extensively published.](#)

**Hit-Finding Strategy.** The starting point was a weak activator of innate immune signaling and effector activity, [G10, identified in a high-throughput in vitro screen of 51,632 compounds](#). The high-throughput assay was designed to identify compounds that would stimulate IFN-dependent as well as IRF3-dependent transcription. Through several biochemical assay screens, G10 was determined to activate IRF3 transcriptional activity via a STING-dependent pathway, without direct activation of STING by G10.

**Lead Optimization.** Upon re-examination of the structure of G10, the researchers noticed chemical similarities with STING agonists currently under development, and thus decided to test the activity of G10 with HAQ STING variants, R232 and H232. G10 showed activation for these variants, suggesting the potential for STING agonism. G10 was then used as a structural starting point for analog synthesis, resulting in [“compound 5”](#), which showed enhanced potency for STING R232. Further structure-activity relationship (SAR) studies identified an oxindole core structure, resulting in [“compound 53”](#), which demonstrated robust on-target functional activation of STING (human EC<sub>50</sub> 185 nM).

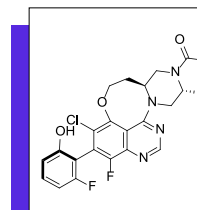


**Binding Mode.** [Structural data](#) reported by UT Southwestern scientists suggests that “compound 53” induces oligomerization and subsequent activation of STING through a unique mechanism that allows both the compound and cGAMP to bind, leading to a stronger STING activation not afforded by either modulator alone.

**JDQ443 | KRAS<sup>G12C</sup>**

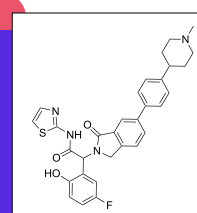
oral KRAS<sup>G12C</sup> inhibitor  
Ph. III candidate for NSCLC  
from de novo SBDD in SWII pocket  
*Cancer Discov.*

Novartis, Basel, CH

**AZD4625 | KRAS<sup>G12C</sup>**

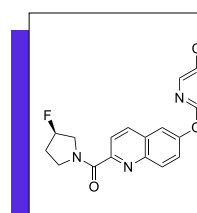
oral KRAS<sup>G12C</sup> inhibitor  
oral efficacy in xenograft mice  
from literature starting point and SBDD  
*J. Med. Chem.*

AstraZeneca, Cambridge, UK

**BJJ-09-063 | EGFR**

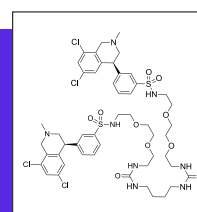
allosteric mutant-EGFR inhibitor  
in vivo efficacy in osimertinib-resistant  
xenograft models  
from opt. of prev. disclosed EGFR inhibitor  
*Nat. Cancer*

Dana-Farber Cancer Institute, Boston, MA

**ABBV-318 | Na<sub>v</sub>1.7/1.8**

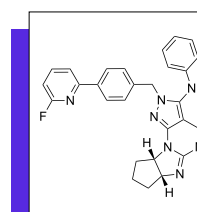
oral CNS-penetrant Na<sub>v</sub>1.7/1.8 blocker  
in vivo efficacy in rodent pain models  
electrophysiology-based HTS and opt.  
*Bioorg. Med. Chem.*

AbbVie, North Chicago, IL

**tenapanor | NHE3**

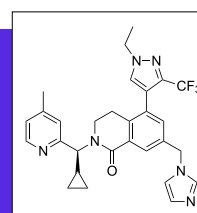
oral gut-restricted Na<sup>+</sup>/H<sup>+</sup> exchanger inhibitor  
FDA-approved IBS treatment  
from literature starting point and opt  
*ACS Med. Chem. Lett.*

Ardelyx Inc., Fremont, CA/Waltham, MA

**lenrispodun (ITI-214) | PDE1**

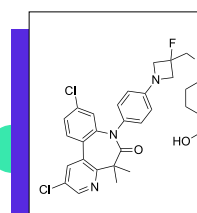
oral, CNS-penetrant, picomolar PDE1 inhibitor  
Ph. I/II in neurology and heart failure  
from literature starting point, LBDD and SBDD  
*Neuropsychopharmacology*

Intra-Cellular Therapies, New York, NY

**compound 41 | WDR5**

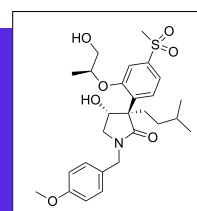
oral WDR5 inhibitor  
pM Ki, nanomolar in cells  
from FBDD, SBDD, and PK opt.  
*J. Med. Chem.*

Vanderbilt University School of Medicine,  
Nashville, TN

**DS69910557 | hPTHR1**

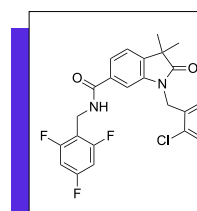
oral hPTHR1 GPCR antagonist  
calcium-lowering activity in rodent  
scaffold-hopping from lit. starting point  
*Bioorg. Med. Chem.*

Daiichi Sankyo, Tokyo, JP

**compound 14 | HIV-1 protease**

potent HIV-1 protease inhibitor  
in vitro activity (IC<sub>50</sub> = 0.0071 μM, EC<sub>50</sub> = 0.86 μM)  
from "pocket-to-lead" virtual screen and SBDD  
*J. Med. Chem.*

Shionogi, Osaka, JP

**compound 53 | STING**

non-nucleotide STING agonist  
novel mechanism for STING activation  
from micromolar HTS hit  
*Nature*

University of Texas Southwestern  
Medica Center, Dallas, TX

**discover together**

**drughunter.com**  
**info@drughunter.com**